

HEAT TRANSFER AND PRESSURE DROP FOR FLUID FLOW
ACROSS A TUBE BANK

By

DON ADAMS

Bachelor of Science

Oklahoma State University

Stillwater, Oklahoma

1962

Submitted to the faculty of the Graduate School of
the Oklahoma State University
in partial fulfillment of the requirements
for the degree of
MASTER OF SCIENCE
May, 1964

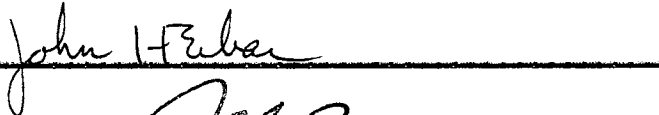
JAN 8 1965

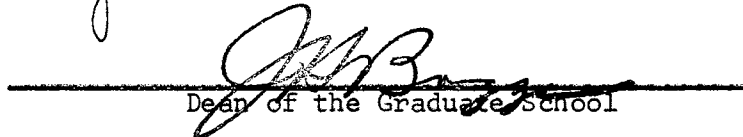
HEAT TRANSFER AND PRESSURE DROP FOR FLUID FLOW
ACROSS A TUBE BANK

Thesis Approved:



Thesis Adviser





Dean of the Graduate School

PREFACE

A significant number of plants for producing non-Newtonian polymers have been built in the past few years, and more will be built in the future. There is a shortage of heat transfer data and pressure drop data for the flow of non-Newtonian fluids across tube banks.

A tube bank was designed in hopes of obtaining heat transfer data and pressure drop data for the flow of non-Newtonian fluids across tube banks. The tube bank was tested experimentally using water and was found to give partially unsatisfactory results. Design details and results of the experimental runs are presented in this thesis.

I received aid from a number of individuals during the course of this project. Dr. Kenneth J. Bell was very helpful in the formulation and testing of the design. Messrs. Gene E. McCroskey, Preston Wilson, and Arlin Harris gave many helpful suggestions and much aid in the construction of the apparatus. I wish to also express my gratitude to my wife, Barbara, who typed this thesis and gave me encouragement.

I am indebted to the Federal Department of Health, Education, and Welfare which provided me with a National Defense Education Act Fellowship during the course of this study. I am also indebted to the Office of Engineering Research, Oklahoma State University, which provided the institutional research funds for purchasing the necessary equipment.

TABLE OF CONTENTS

Chapter	Page
I. INTRODUCTION	1
II. FLUID BEHAVIOR CLASSIFICATION.	3
Newtonian Fluids.	3
Non-Newtonian Fluids.	3
Classification of Non-Newtonian Fluids.	5
III. LITERATURE SURVEY.	8
Newtonian Fluid Flow Across Tube Banks.	8
Non-Newtonian Fluid Flow.	9
IV. EXPERIMENTAL APPARATUS	13
Tube Bank	13
Tube Construction	20
Auxiliary Equipment	22
V. EXPERIMENTAL PROCEDURE	26
Start-Up Procedure.	26
Orifice Calibration	26
Heat Transfer Data Procedure.	26
Pressure Drop Data Procedure.	27
VI. PRESENTATION AND DISCUSSION OF RESULTS	28
Heat Transfer Results	28
Pressure Drop Results	35
VII. CONCLUSIONS AND RECOMMENDATIONS.	40
Conclusions	40
Recommendations	40
A SELECTED BIBLIOGRAPHY	41
APPENDIX A. DEFINITION OF SYMBOLS.	42
APPENDIX B. EXPERIMENTAL AND CALCULATED DATA	45
APPENDIX C. ORIFICE CALIBRATION.	54

LIST OF TABLES

Table	Page
I. Heat Transfer Rate Results From Design B.	29
II. Low Heat Input Results for Design C	32
III. Comparison of Low Heat Input Results with Grimison Correlation	33
IV. High Heat Input Results for Design C.	34
V. Comparison of High Heat Input Results with Grimison Correlation	36
VI. Pressure Drop Results	37
VII. Comparison of Friction Factor Results with Grimison Correlation	39
VIII. Heat Transfer Raw Data for Design B	46
IX. Low Heat Input Raw Data for Design C.	47
X. High Heat Input Raw Data for Design C	48
XI. Tube Bank Pressure Drop Raw Data.	52
XII. Orifice Calibration Data.	55

LIST OF FIGURES

Figure	Page
1. Shear Diagram.	4
2. Photographs of Apparatus	14
3. Flow System.	15
4. Top View of Tube Bank.	16
5. Side View and End View of Tube Bank.	17
6. Tube Bank Photographs.	18
7. Flanges Holding Tube Bank.	19
8. Tube Design A.	21
9. Tube Design B.	23
10. Electrical Circuit Diagram	24
11. Friction Factor Versus Reynolds Number for a Tube Bank Having a Rotated Square Tube Configuration and a Pitch Ratio of 1.33	38
12. Orifice Calibration.	57

CHAPTER I

INTRODUCTION

Heat exchange equipment makes up a significant portion of the investment for many chemical plants. The heat exchange equipment is often larger than is required due to the lack of reliable heat transfer coefficients. Predicted heat transfer coefficients for the shell side of shell and tube heat exchangers are often unreliable. A step in the direction of more reliable shell side heat transfer coefficients is the accurate determination of heat transfer coefficients for flow across ideal tube banks.

Pumping equipment is also often oversized due to the lack of reliable pressure drop calculation methods.

A number of new polymers have been developed in the last few years, and more polymers are likely to be developed in the years to come. The behavior of solutions of these polymers is often non-Newtonian.

Little information has been published on the development of heat transfer coefficient and friction factor correlations for the flow of non-Newtonian fluids across tube banks.

The following goals were set for this project:

1. Design an apparatus which may be used to obtain heat transfer coefficients and friction factors for the flow of fluids across tube banks.

2. Test this apparatus for reliability using water and compare results with those presented in the literature.
3. Using the apparatus, obtain heat transfer coefficient and friction factor data for a non-Newtonian fluid.
4. Correlate these data for the non-Newtonian fluid.

Goals 3 and 4 were not reached due to the fact that the apparatus designed did not give reliable heat transfer coefficients for water.

CHAPTER II

FLUID BEHAVIOR CLASSIFICATION

Newtonian Fluids

A Newtonian fluid is one for which the following equation applies:

$$\tau = \mu \frac{du}{dy} \quad (1)$$

The proportionality constant, μ , is known as the viscosity. The velocity gradient, $\frac{du}{dy}$, is called the shear rate, and τ is called the shearing stress.

The viscosity, defined in the above equation, is dependent on the temperature, pressure, and the fluid under consideration. It does not depend upon the rate of shear. If shearing stress and shear rate are plotted at constant temperature and pressure, a straight line is obtained (see Figure 1) passing through the origin. The slope of this straight line is the viscosity.

Non-Newtonian Fluids

A fluid which does not obey Equation 1 is called a non-Newtonian fluid.

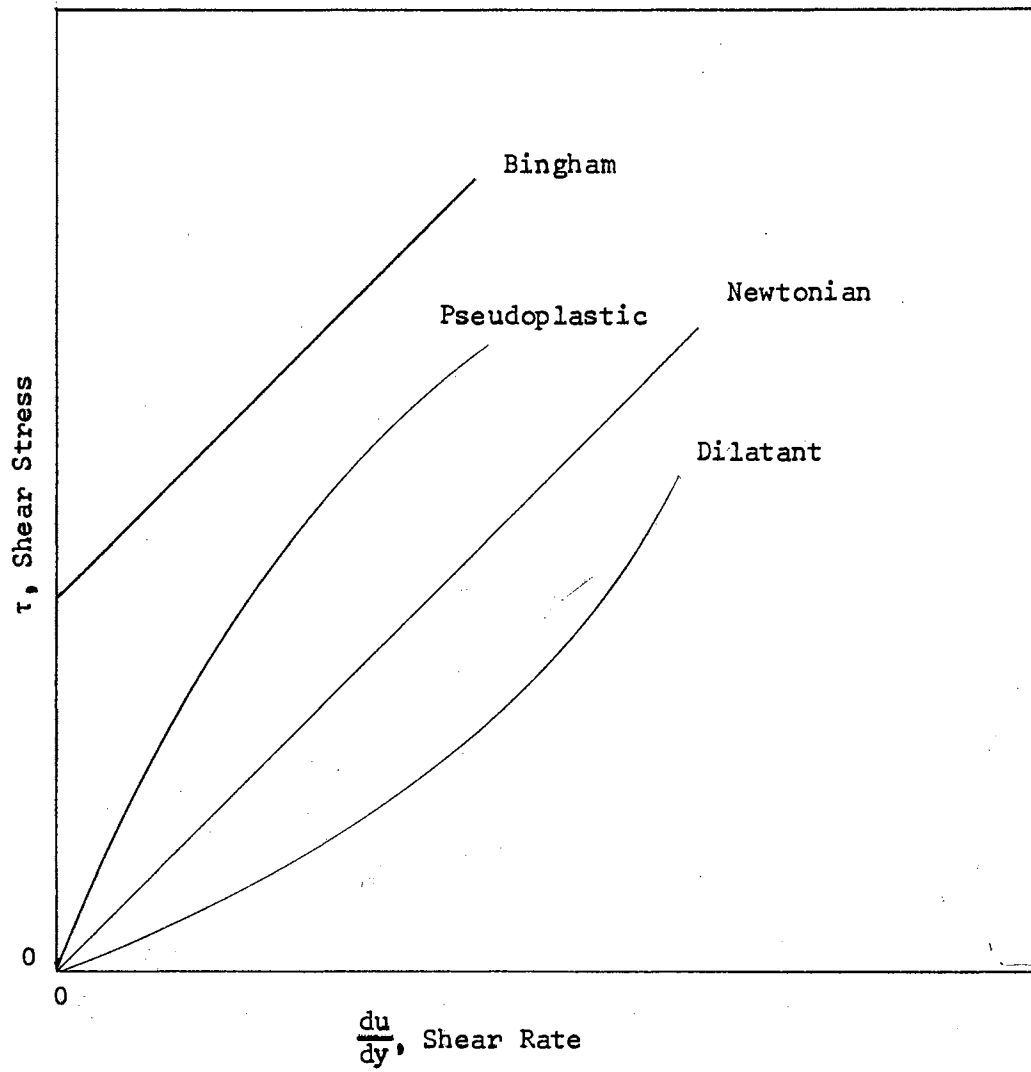


Figure 1. Shear Diagram

Classification of Non-Newtonian Fluids

There are three broad classes of non-Newtonian fluids (1). These are

1. Time-independent
2. Time-dependent
3. Viscoelastic

Time-Independent Non-Newtonian Fluids

For these fluids, the shear stress does not depend upon the duration of the shear. These fluids are usually subdivided into three types. These are

1. Bingham plastics
2. Pseudoplastic fluids
3. Dilatant fluids

The shear curve for each of these three types of time-independent fluids is presented in Figure 1.

Bingham Plastic. This type of fluid has a linear shear curve; however, the shear curve does not intersect the axis at the origin but intersects the axis at a fixed point τ_y , which is an initial shear stress which must be exerted on the fluid to make it flow. This fluid is characterized by the following equation (1):

$$\tau - \tau_y = \mu_B \left(\frac{du}{dy} \right) \quad (2)$$

The term, μ_B , is called the plastic viscosity or coefficient of rigidity.

Pseudoplastic. The shear curve for this type of fluid passes

through the origin, and its slope decreases with increasing shear rate (see Figure 1). The shear curve of this type of fluid tends to become linear at very high shear rates. The shear curve for a pseudoplastic fluid can often be represented by the following equation (1):

$$\tau = K \left(\frac{du}{dy} \right)^n \quad (3)$$

The constant, n , is an indication of the deviation from non-Newtonian behavior, and K is a measure of the viscosity of the fluid. The constant, n , equals 1.0 for a Newtonian fluid. Pseudoplastic fluids are often referred to as power law fluids, since their shear curve can often be represented by Equation 3. For these fluids, the constant, n , must be between 0 and 1.

Dilatant Fluids. The shear curve for these fluids passes through the origin, and its slope increases with increasing shear rate (see Figure 1). The behavior of these fluids can be represented by the power law equation (Equation 3); however, the constant, n , for these fluids is greater than one since the slope of the shear curve increases with increasing shear rate.

Time-Dependent Non-Newtonian Fluids

For these fluids, the apparent viscosity depends upon the length of time during which the shear has been applied. These fluids are subdivided into two types. These are

1. Thixotropic
2. Rheopectic

Thixotropic. The apparent viscosity decreases with the time of shear (1).

Rheopectic. The apparent viscosity increases with the time of shear (1).

Viscoelastic Fluids. These fluids exhibit both viscous and elastic properties (1). The energy applied to such a fluid is stored as potential energy in addition to being dissipated as heat by the viscous forces. An equation to describe such behavior should be a combination of Newton's viscosity law for fluids and Hooke's law for elastic materials (1).

It is highly possible that a particular fluid will not fall into a particular classification for all shear rates. A fluid may be time-dependent for a short period of time and become time-independent after a long period of time.

CHAPTER III

LITERATURE SURVEY

Newtonian Fluid Flow Across Tube Banks

Convection heat transfer rate and flow resistance data for the flow of gases over tube banks were obtained by Pierson (2) to determine the effect of varying the spacing of tubes of identical size. Measurements were made for both in-line and staggered tube arrangements. The tubes were electrically heated. The Reynolds number, $D_o G_m/\mu$, range was from 2,000 to 40,000. These measurements showed that the heat transfer rate and flow resistance are significantly affected by variations in the tube spacing.

Investigations were made by Huce (3) to determine the effect of tube size on the heat transfer coefficient and the pressure drop. These tube banks had both in-line and staggered tube arrangements. Condensing steam and water were used in the tubes, and the Reynolds number range was from 2,000 to 70,000. The heat transfer coefficient was found to be proportional to the 0.61 power of the Reynolds number.

The data obtained by Pierson (2) and Huce (3) were analyzed by Grimison (4) in hope of obtaining a heat transfer correlation and a friction factor correlation suitable for commercial use. The investigation by Grimison (4) covered Reynolds numbers from 2,000 to 40,000. The work by Grimison (4) indicated that the heat transfer rate is proportional

to approximately the $2/3$ power of the Reynolds number. Grimison (4) also presented graphical correlations of the friction factor as a function of Reynolds number, tube spacing transverse to flow, tube spacing in the direction of flow, and tube diameter.

Data for the flow of oil across unbaffled tube banks has been presented by Bergelin, Colburn, and Hull (5). The effect of tube size, pitch ratio, and the number of tube rows were investigated. Most of these data are for the laminar flow region. The Reynolds number ranged from 1.4 to 875.

Bergelin, Brown, and Doberstein (6) have presented an extension of the previous work. Pressure drop and heat transfer rate data for flow of a light oil across five tube banks having five different tube arrangements were obtained. The Reynolds number ranged from 25 to 10,000. The data for the lower Reynolds numbers are in good agreement with those presented by Bergelin, Colburn, and Hull (5). The data for the higher Reynolds numbers are in generally good agreement with the data of Grimison (4).

Non-Newtonian Fluid Flow

Metzner (7) has presented a generalized form of the Reynolds number to be applied to power law non-Newtonian fluids. Metzner substitutes $V = 4Q/\pi D^2$ and rearranges the following expression derived by Rabinowitsch (8) for a time-independent fluid in laminar flow in a conduit:

$$+ \left(\frac{du}{dy} \right)_w = 3 \left(\frac{8Q}{\pi D^3} \right) + \frac{D \Delta P}{4L} \frac{d (8Q/\pi D^3)}{d (D \Delta P/4L)} \quad (4)$$

The substitution of $V = 4Q/\pi D^2$ and rearrangement gives

$$\left(\frac{du}{dy}\right)_w = 3/4 \left(\frac{8V}{D}\right) + \frac{1}{4} \left(\frac{8V}{D}\right) \frac{d \ln (8V/D)}{d \ln (D \Delta P/4L)} \quad (5)$$

Metzner then makes the following substitution:

$$\frac{1}{n'} = \frac{d \ln (8V/D)}{d \ln (D \Delta P/4L)} \quad (6)$$

Rearrangement of Equation 5 then gives

$$\left(\frac{du}{dy}\right)_w = \frac{3n' + 1}{4n'} \left(\frac{8V}{D}\right) \quad (7)$$

The constant, n' , can now be found from the slope of a plot of $\ln (8V/D)$ against $\ln (D \Delta P/4L)$. Integration of Equation 6 for a constant n' gives

$$\frac{D \Delta P}{4L} = K' \left(\frac{8V}{D}\right)^{n'} \quad (8)$$

where K' is also a constant. The constants K' and n' have been found to be constant over wide ranges of $8V/D$ (7). Metzner substitutes the relationship for $\frac{D \Delta P}{4L}$ in Equation 8 into the following friction factor equation:

$$f = \left(\frac{D \Delta P}{4L}\right) \frac{\rho V^2}{2 g_c} \quad (9)$$

This gives

$$f = \frac{16\gamma}{D^{n'} V^2 - n' \rho} \quad (10)$$

Letting $f = 16/Re$ now gives the following generalized Reynolds number:

$$Re = \frac{D^{n'} V^2 - n' \rho}{\gamma} \quad (11)$$

$$\gamma = g_c K' g^{n'} - 1 \quad (12)$$

This generalized Reynolds number has given very good correlation results for the Fanning friction factor for flow inside circular tubes (7).

The Reynolds number for flow across tube banks is

$$Re = \frac{D_o V_m \rho}{\mu} \quad (13)$$

By analogy with Equations 11 and 13, the generalized Reynolds number for non-Newtonian fluid flow across a tube bank is proposed to be

$$Re = \frac{D_o^{n'} V_m^{2-n'} \rho}{\mu} \quad (14)$$

The proposed form given in Equation 14 will reduce to the Newtonian form of Equation 13 for $n' = 1$ as for Newtonian flow.

Acrivos, Petersen, and Shah (9) have presented data for heat transfer from a single cylinder to a power law non-Newtonian fluid. They have presented plots of theoretical heat transfer coefficients from boundary layer theory as a function of the generalized Reynolds number. They have also presented plots of the experimental heat transfer coefficients against the theoretical heat transfer coefficients. The experimental and calculated heat transfer coefficients agreed fairly well.

The friction factor is used for correlation of the pressure drop data obtained in this work. This friction factor is defined by the following equation:

$$f = \frac{\Delta P g_c \rho}{2 G^2 N} \quad (15)$$

For the heat transfer data, the Nusselt number, $h D_o/k$, was to be correlated as a function of the generalized Reynolds number defined by Equation 11. It was hoped that the friction factor and Nusselt number would be the same as for Newtonian fluids with the non-Newtonian behavior being taken into consideration in the generalized Reynolds number.

CHAPTER IV

EXPERIMENTAL APPARATUS

The fluid being circulated was pumped from a holding barrel into a 1 1/2 inch schedule 40 pipe where it flowed through an orifice plate, then the tube bank, and back into the holding barrel (see Figures 2 and 3).

Tube Bank

The walls of the tube bank were made of brass 3/16 inch thick and were soldered together. The tube bank was 6 inches long by 2 13/16 inches by 2 7/8 inches (see Figures 4, 5, and 6). The tube bank consisted of ten rows of 3/8 inch O.D. by 2 7/8 inch long brass tubes which were soldered into the tube bank walls. The tubes were in a rotated square configuration, and the pitch-to-tube diameter ratio was 1.333; that is, the center-to-center distance between adjacent tubes in the rotated square was 1/2 inch (see Figure 4). Half-tubes were soldered to the tube bank walls at places where there was space for only half of a tube in order to reduce wall effects (see Figure 4).

Two 1/4 inch O.D. copper tubing pressure taps were connected to the tube bank (see Figure 4) to measure the pressure drop across the tube bank.

The tube bank was held in place by two 2-inch pipe flanges. The flanges were machined so that the tube bank would fit into the flanges (see Figure 7). Cork gaskets, 1/16 inch thick, were

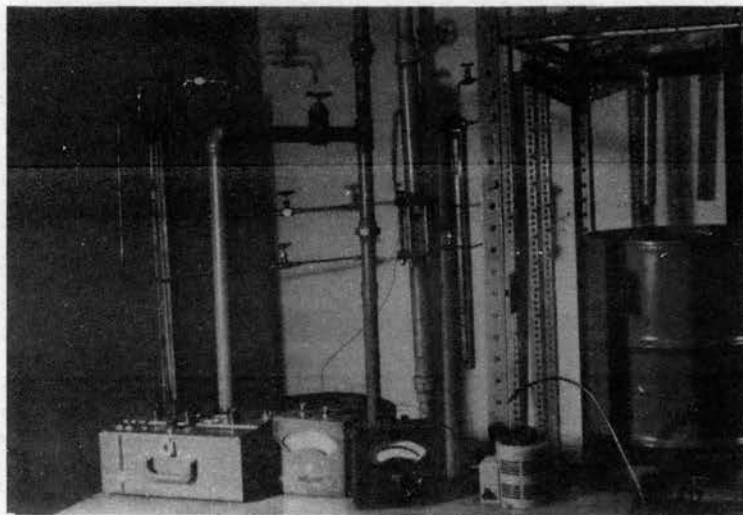
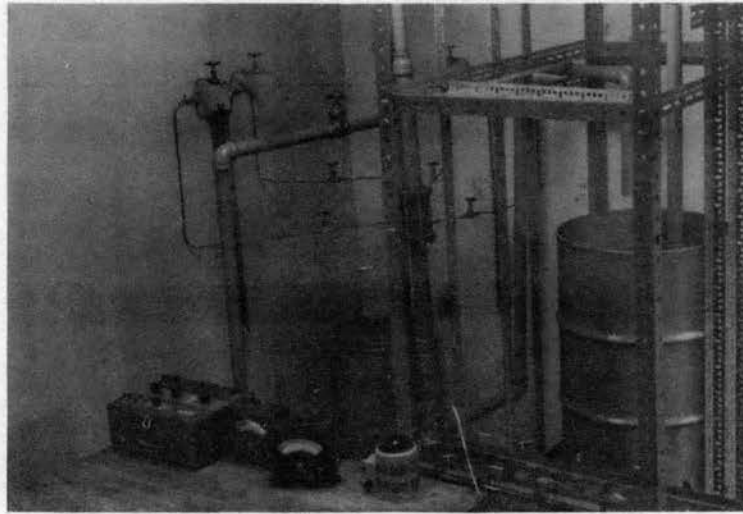


Figure 2. Photographs of apparatus

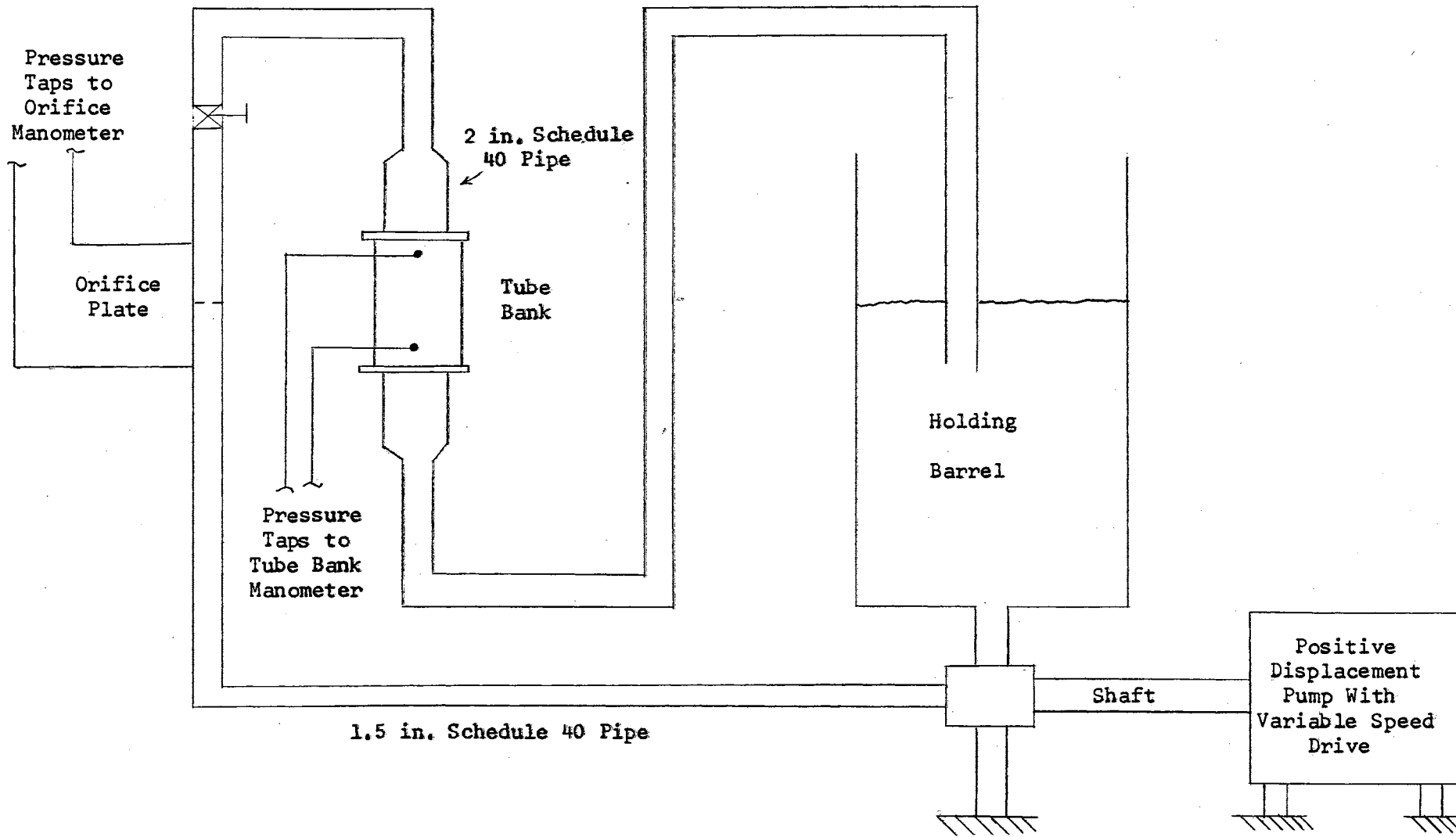


Figure 3. Flow System

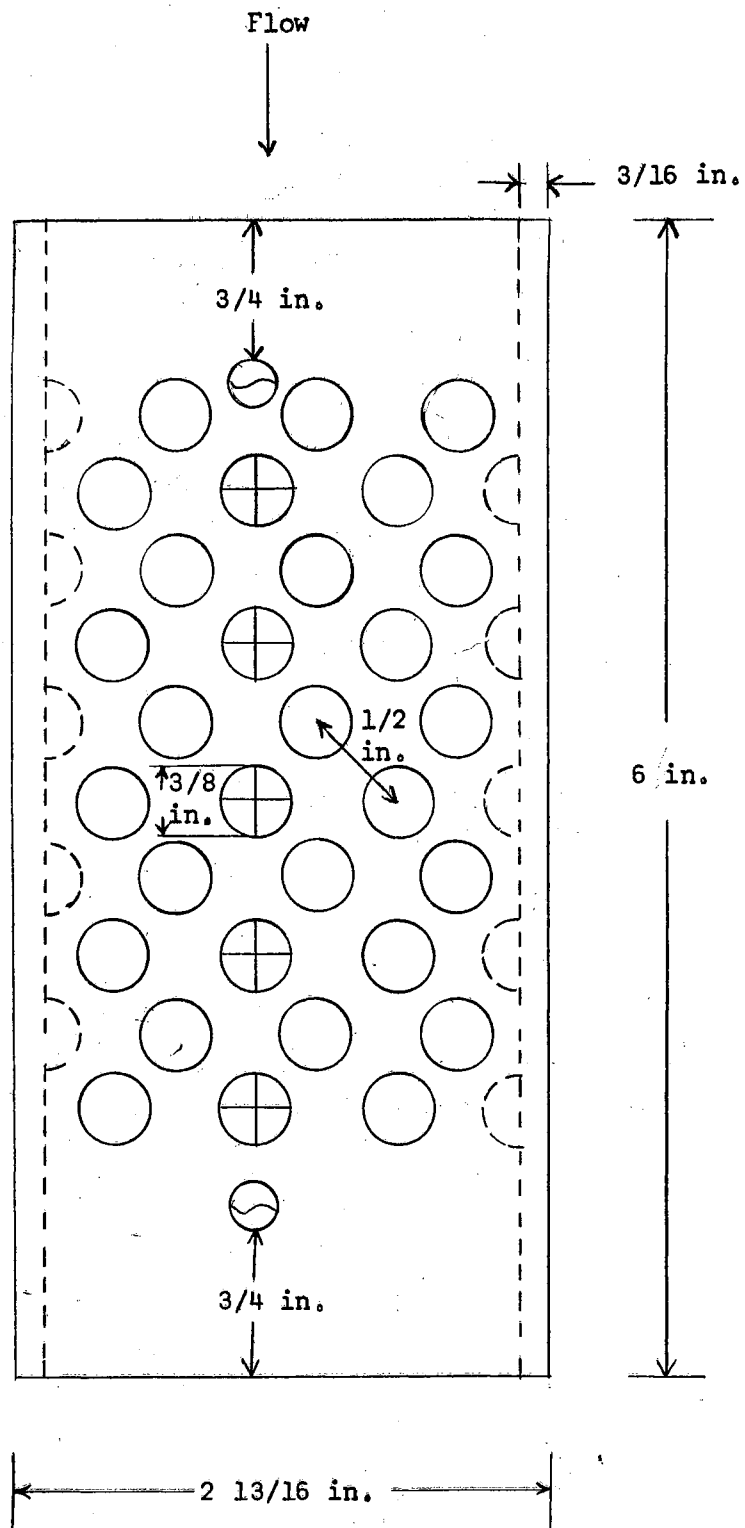


Figure 4. Top View of Tube Bank

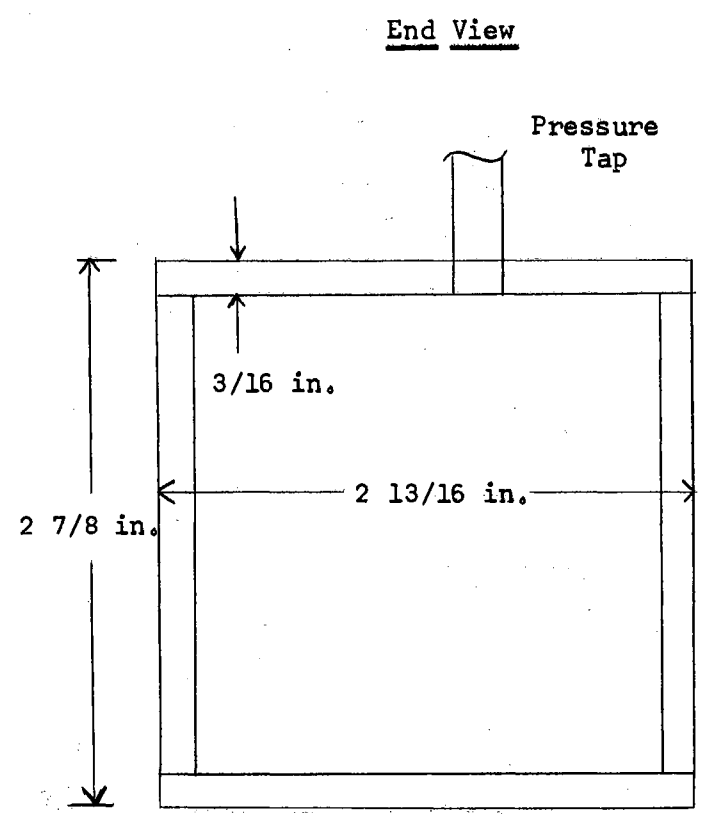
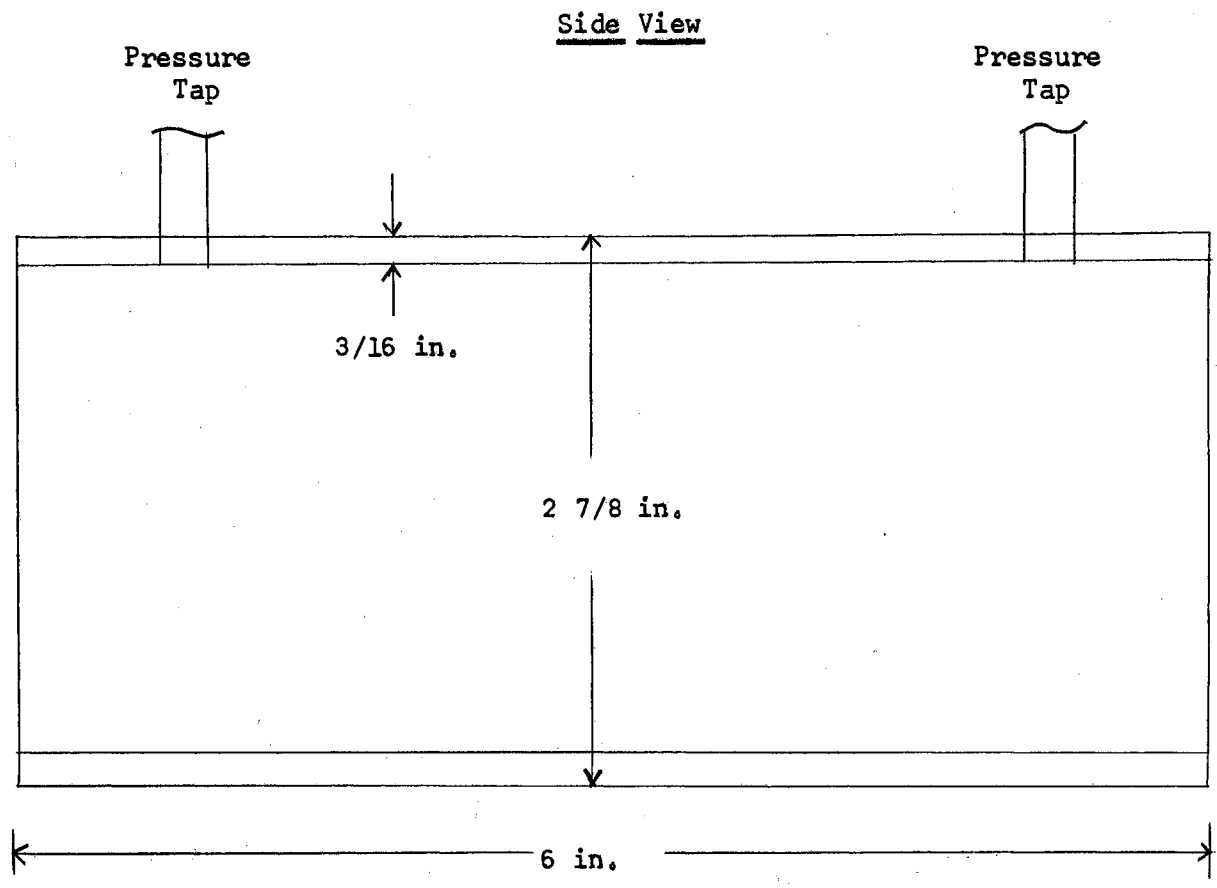


Figure 5. Side View and End View of Tube Bank

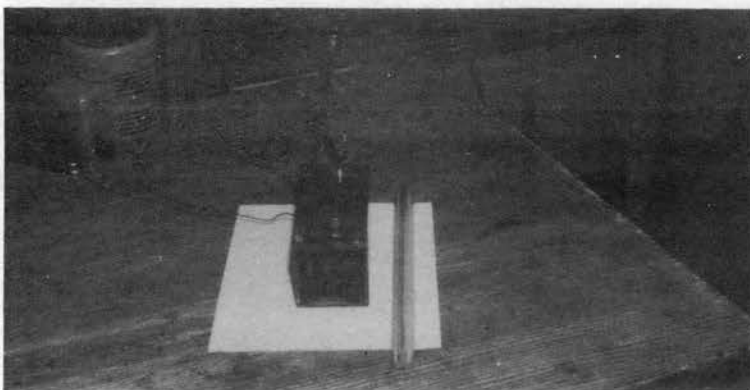
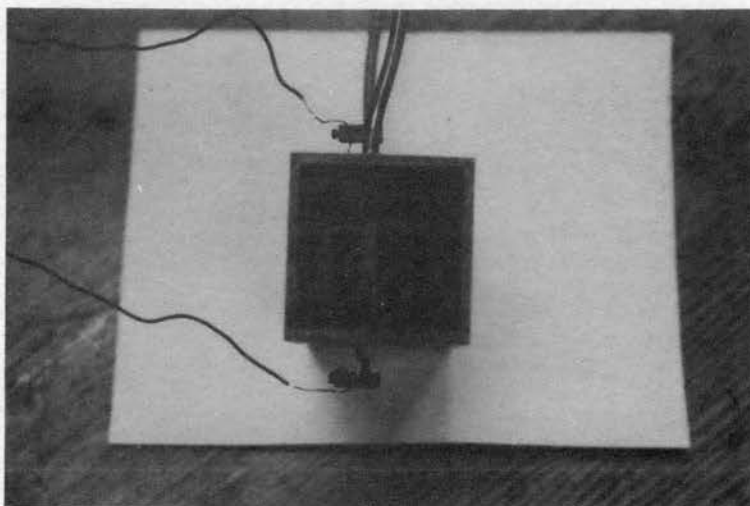
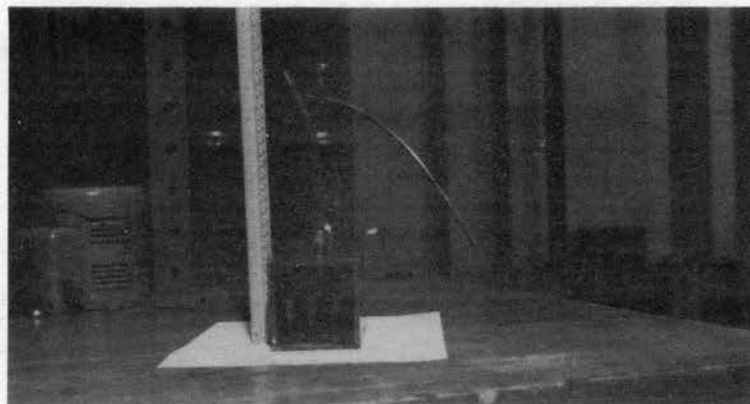


Figure 6. Tube Bank Photographs

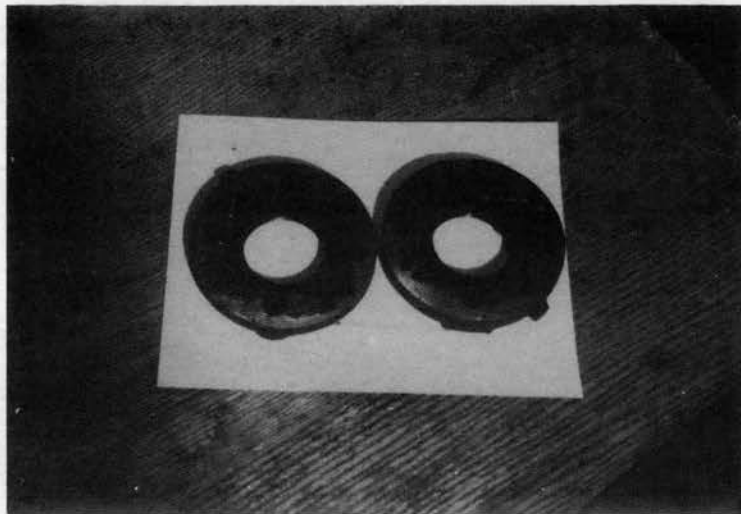


Figure 7. Flanges Holding Tube Bank

inserted between the tube bank and the flange surface to prevent leakage.

A piece of screen was also placed ahead of the tube bank to smooth the flow and to prevent foreign material from flowing into the tube bank.

Tube Construction

All of the tubes except five were of brass rod $3/8$ inch O.D. by $2\ 7/8$ inches long. Five of the tubes were specially made so that an electrical current might be passed through them in order to generate a known amount of heat. Three tube designs were considered; however, only two were used experimentally.

Design A

The heating element consisted of a $1/8$ inch O.D. graphite rod surrounded with a $1/16$ inch thick layer of insulating cement (see Figure 8). Around the insulating cement was the $1/16$ inch thick wall of the brass tube. A small hole was located in the center of the graphite rod for inserting a thermocouple to measure the temperature at the center of the tube. After attempting to construct an experimental tube, this design was abandoned due to the difficulty involved in getting the insulating cement between the graphite and the tube wall. This difficulty occurred because the space between the graphite rod and the tube wall was too small for one to be able to insert the cement. Also, the electrical resistance of the graphite rod was so low that large currents (10 to 50 amperes) would be required to produce the desired amount of heat.

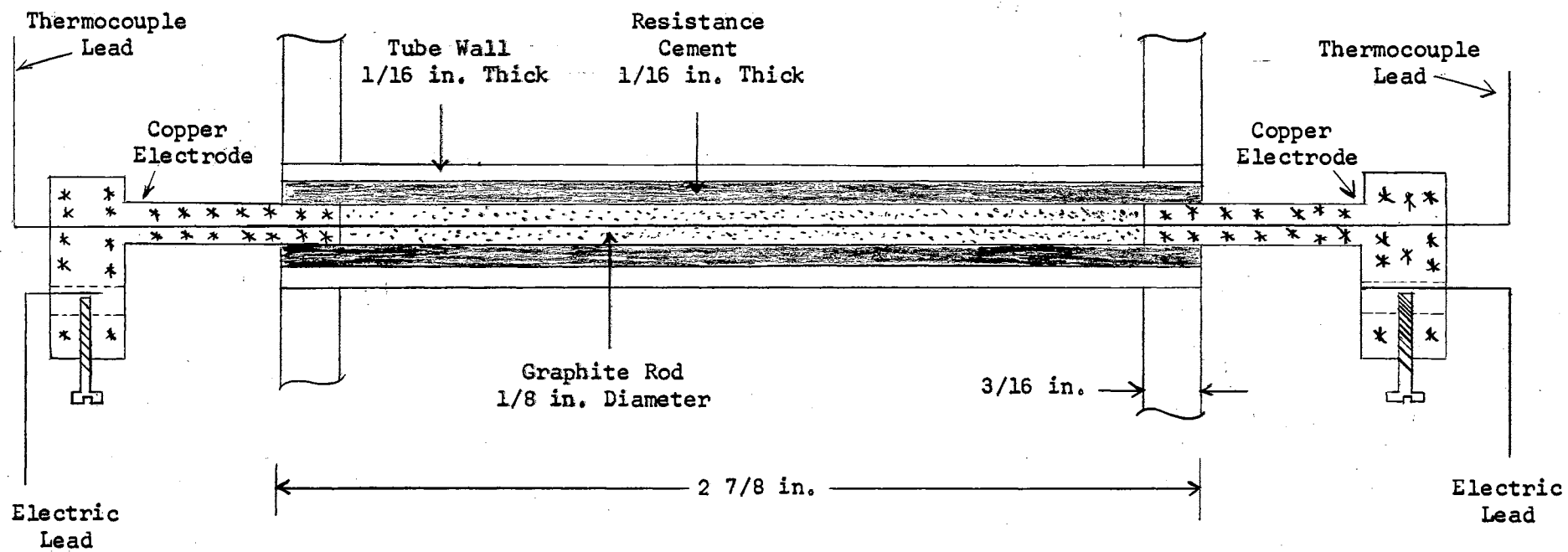


Figure 8. Tube Design A

Design B

The heating element consisted of Thermon Standard heat transfer cement packed in a zircon tube having an inside diameter of 1/8 inch and an outer diameter of 5/16 inch (see Figure 9). The electrical resistivity of this type of element is much larger than that of the graphite; therefore, much lower currents were required for Design B. The zircon tube was surrounded by the brass tube wall. A thermocouple was placed between the zircon and the brass wall by cutting a slot approximately 1/16 inch wide and 1/16 inch deep into the wall of the zircon tube. It was possible to rotate the zircon tube; therefore, it was possible to measure the heat transfer rate at different radial positions on the tube.

Design C

This design was the same as Design B except there was no slot in the zircon tube, because the thermocouple was soldered into the tube wall from the outside of the tube.

Auxiliary Equipment

The pump was a Moyno 1L6, type CDQ, positive displacement pump, and it was driven by a three-horsepower electric motor. A variable-speed drive attached to the motor was used to control the flow rate.

A 42-gallon barrel was used to hold the fluid being circulated.

Voltage for the heated tubes was controlled by a Powerstat. A 0 - 1 ampere A.C. ammeter and a 0 - 50 volt voltmeter were used to measure the heat supplied to the tubes at low-heat inputs. At the high-heat inputs, a 0 - 5 ampere A.C. ammeter and a 0 - 150 volt voltmeter were used. A diagram of the electrical circuit is presented in Figure 10 on page 24.

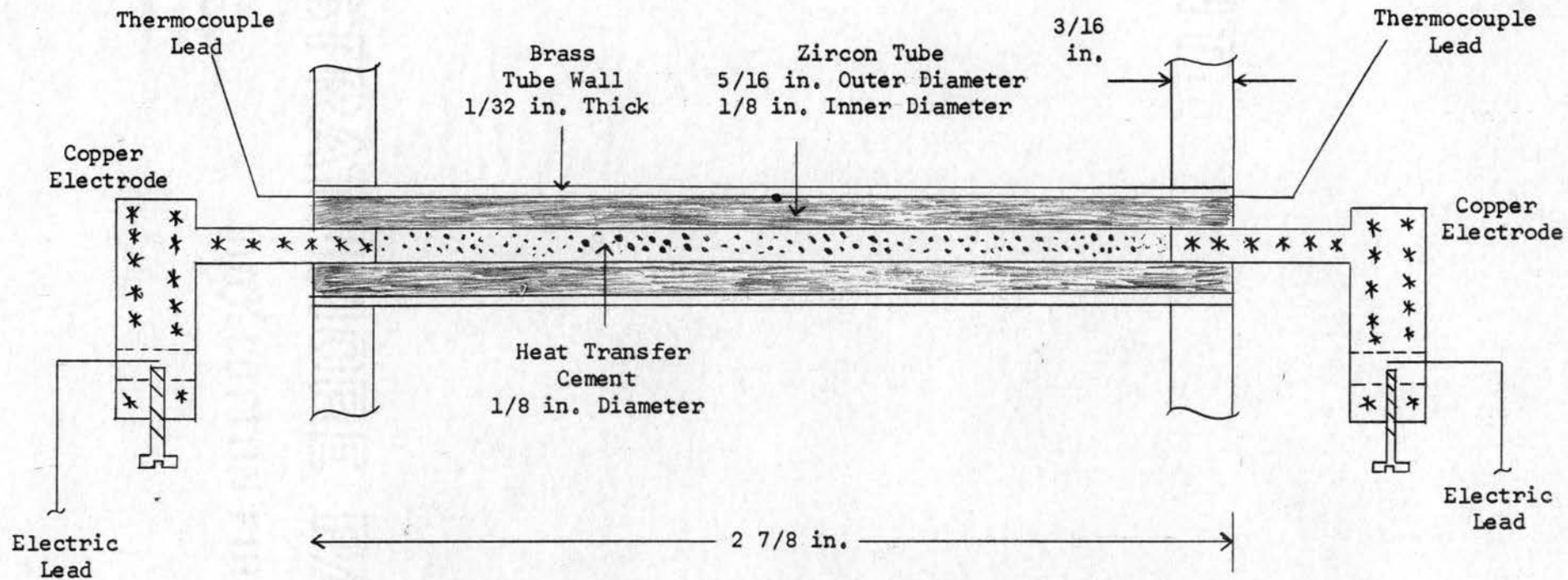


Figure 9. Tube Design B

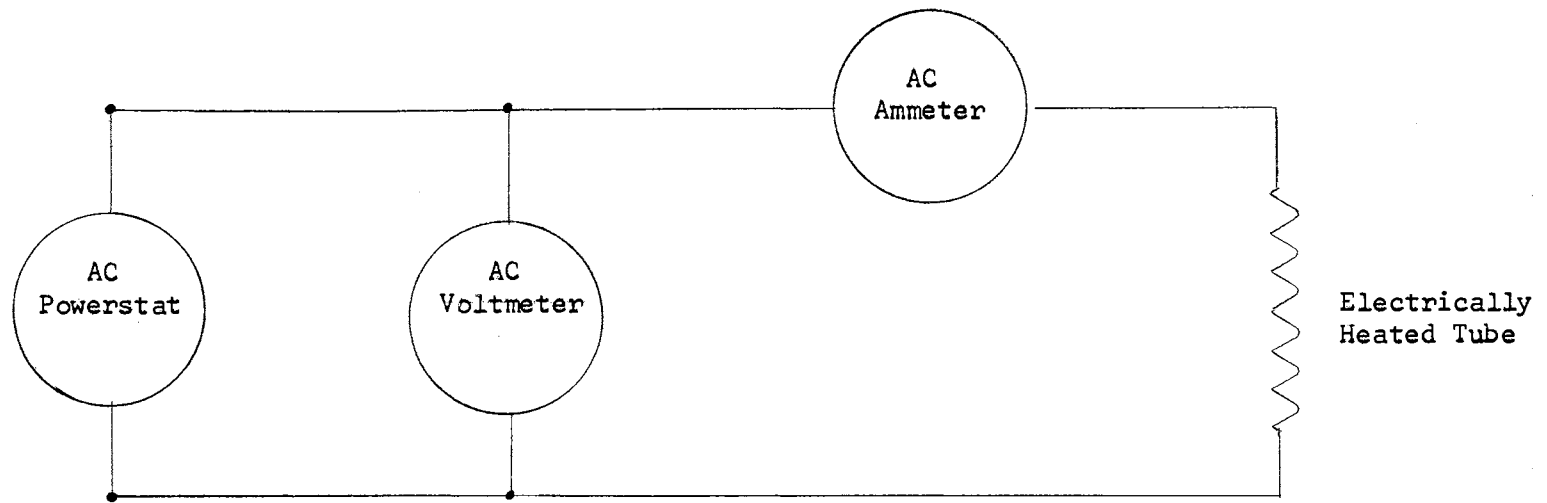


Figure 10. Electrical Circuit Diagram

Copper-constantan thermocouples (24 gauge) were used to measure the bulk-fluid temperature and the tube temperatures. A selector switch was used to select the proper thermocouple, and the thermocouples were connected to a portable Leeds and Northrup potentiometer. Thermocouple calibration tables accompanying the potentiometer were used for thermocouple calibration.

An orifice plate with a diameter of $23/32$ inch and a thickness of $1/8$ inch was used to measure the flow rate (see Figure 3). The orifice pressure taps were of $1/4$ inch O.D. copper tubing and were connected to a 30-inch, U-tube manometer containing mercury.

The pressure taps for measuring the tube bank pressure drop were of $1/4$ inch copper tubing and were connected to a 30-inch, U-tube manometer containing carbon tetrachloride. A very small amount of iodine was dissolved in the carbon tetrachloride in order to give it a red color

CHAPTER V

EXPERIMENTAL PROCEDURE

Start-Up Procedure

The holding barrel was filled about half full of water. This was done several hours before any runs were made to allow the water to come to room temperature.

The pump speed was turned to the lowest setting, and the pump was started.

The air was then bled from the lines to the manometers through valves located above the manometer. These valves were allowed to remain open for about 30 minutes.

Orifice Calibration

The orifice pressure drop was recorded. A stop watch was used to measure the time necessary for 21 pounds of water to flow into a bucket. Several of the time measurements were made, and the average time required was recorded.

Heat Transfer Data Procedure

The Powerstat voltage was set to give the desired heat input to the heated tube. The potentiometer was then used to measure the voltage for the thermocouple in the bulk fluid and for the thermocouple in the

heated tube. When the potentiometer readings for the thermocouple in the tube and for the thermocouple in the bulk fluid became constant, they were recorded. The manometer reading was also checked to see that it remained constant. It usually took less than one minute for these readings to become constant. The voltmeter reading, ammeter reading, and orifice manometer reading were then recorded. This procedure was carried out for each flow rate.

Pressure Drop Data Procedure

The temperature of the water was recorded, and the orifice and tube bank manometer readings were then recorded for each flow rate.

CHAPTER VI

PRESENTATION AND DISCUSSION OF RESULTS

Heat Transfer Results

Heat transfer results were obtained for both tube designs B and C.

Design B

These tubes were designed in such a way that the heat transfer coefficient at radial positions besides the forward stagnation point could be obtained by rotating the slotted zircon tube to put the tube thermocouple at the desired point. Heat transfer data were obtained at angles of 0° , 90° , 180° , 270° , and 315° in a clockwise direction from the forward stagnation point. These data were found to be reproducible at a given angle.

The results obtained for this tube design are presented in Table I.

The following discrepancies were found in the results:

1. There was no significant variation of the heat transfer coefficient with flow rate.
2. The heat transfer coefficients did not vary with radial position as one would expect.
3. The heat transfer coefficients were much lower than expected. According to the work of Grimison (4),

TABLE I
HEAT TRANSFER RATE RESULTS FROM DESIGN B

Run Number	θ	Q Btu/hr.	T _{tube} °F	T _{water} °F	ΔT °F	V _m ft./sec.	Re	h Btu/hr.-ft. ² -°F
1	0°	20.4	87.5	75.5	12.0	5.64	21,100	83.3
2	0°	20.1	87.3	75.5	11.8	3.02	11,300	83
3	0°	20.2	87.5	76.0	11.5	2.73	10,200	85.6
4	90°	18.13	89.1	77.5	11.6	5.64	21,100	76.3
5	90°	18.13	88.8	77.5	11.3	4.34	16,300	78.3
6	90°	18.13	89.1	77.5	11.6	2.73	10,200	76.3
7	180°	18.0	85.5	77.0	8.5	3.79	14,200	103
8	180°	17.75	85.4	77.0	8.4	4.42	16,600	103
9	180°	17.4	85.2	77.0	8.2	2.73	10,200	103
10	270°	16.1	80.7	77.4	3.3	2.73	10,200	238
11	270°	16.25	81	77.5	3.5	4.52	17,000	229
12	270°	16.36	81	77.5	3.5	5.64	21,100	231

θ = angle from forward stagnation point in the clockwise direction

TABLE I (Concluded)

HEAT TRANSFER RATE RESULTS FROM DESIGN B

Run Number	θ	Q Btu/hr.	T _{tube} °F	T _{water} °F	ΔT °F	V _m ft./sec.	Re	h Btu/hr.-ft. ² -°F
13	315°	22.9	83.3	75.5	7.8	1.46	5,500	143
14	315°	22.7	82.7	75.5	7.2	2.91	11,000	154
15	315°	21.9	81.2	75.5	6.7	4.33	16,300	160
16	315°	21.6	81.8	75.5	6.3	5.64	21,100	167

θ = angle from forward stagnation point in the clockwise direction

they should have been between 2,000 and 3,000 Btu/hr.-ft.²-°F.

These three discrepancies may be attributed to a layer of air between the outer surface of the zircon tube and the inner surface of the brass tube. For a heat transfer rate of 20 Btu per hour and an air gap of 0.01 inch, the temperature difference across the air gap would be 54°F.

Due to this air gap, the tube thermocouple which was in the air gap was giving a temperature significantly different from the tube wall temperature. The thickness of the air gap varied with radial position because neither the brass tube nor the zircon tube was perfectly round. This caused the unexpected variation of the heat transfer coefficient with position.

With this tube design, the tube thermocouple could not be put in good contact with the tube wall; therefore, Design C with the thermocouple soldered into the tube wall from the outside was devised.

Design C

Unlike Design B, this design did not allow one to investigate the radial variation of the heat transfer coefficient.

The set of results presented in Table II was obtained for the first heated tube with the tube thermocouple at the forward stagnation point. This set of results agrees more favorably with the correlation of Grimison (4) as shown in Table III; however, the coefficients are still too low.

Results obtained at higher heat inputs gave apparent heat transfer coefficients which seemed to be too high due to heat being conducted from the heated tube to the rest of the tube bank and to the atmosphere. The results obtained at the higher heat inputs are presented in Table IV

TABLE II

LOW HEAT INPUT RESULTS FOR DESIGN C

Run Number	Q Btu/hr.	T _{tube} °F	T _{water} °F	ΔT °F	V _m ft./sec.	Re	h Btu/hr.-ft. ² -°F
17	96.6	72.4	69.7	2.7	4.50	16,000	1,730
18	96.6	72.6	70.5	2.1	5.7	20,300	2,250
19	96.7	74.0	71.1	2.9	4.12	14,800	1,650
20	94.8	76.8	71.8	5.0	2.68	9,800	935

TABLE III
COMPARISON OF LOW HEAT INPUT RESULTS WITH
GRIMISON CORRELATION (4)

Re	h (This Work) Btu/hr.-ft. ² -°F	h (Grimison) Btu/hr.-ft. ² -°F	Percent Difference
16,000	1,730	2,300	-29.1
20,300	2,250	2,490	-9.62
14,800	1,650	2,240	-26.3
9,800	935	1,940	-51.8

TABLE IV

HIGH HEAT INPUT RESULTS FOR DESIGN C

Run Number	Q Btu/hr.	T _{tube} °F	T _{water} °F	ΔT °F	V _m ft./sec.	Re	h Btu/hr.-ft. ² -°F
21	294	82.2	76.8	5.7	5.4	20,300	2,510
22	683	90.0	78.1	11.9	5.4	20,300	2,800
23	297	84.2	78.4	5.8	5.1	19,200	2,480
24	672	90.4	78.7	11.7	5.1	19,200	2,820
25	322	95.0	78.8	6.2	4.24	15,900	2,550
26	875	93.7	78.9	14.8	4.24	15,900	2,900
27	246	82.9	78.9	7.0	3.16	11,900	3,030
28	552	86.7	78.9	7.8	3.16	11,900	3,450

and are compared with the Grimison correlation (4) in Table V. This table shows that the heat transfer coefficients increased with increasing heat inputs at a constant flow rate. Thus, it is apparent that there were significant heat losses. A thermocouple placed on tubes other than the heated tube showed elevated temperatures which also indicates a significant heat loss. These heat losses are also indicated by the incorrect variation of the heat transfer coefficient with flow rate; that is, the heat transfer coefficients do not decrease with decreasing flow rate.

It was highly desirable to be able to use the higher heat inputs in order to get a larger temperature difference which could be measured more accurately.

Pressure Drop Results

From the pressure drop measurements, the friction factors were calculated. These results are presented in Table VI and in Figure 11. The results are reproducible. The friction factors agree with the values given by Bergelin, Brown, and Doberstein (6) and with the values given by Grimison (4) in the Reynolds number region (4,000 to 8,000) where both of the literature sources apply. The friction factors do not agree with the values given by the Grimison correlation (4) at the higher Reynolds numbers where Bergelin, Brown, and Doberstein (6) do not present data (see Figure 11).

TABLE V
 COMPARISON OF HIGH HEAT INPUT RESULTS WITH
 GRIMISON CORRELATION (4)

Re	Q Btu/hr.	h (This Work) Btu/hr.-ft. ² -°F	h (Grimison) Btu/hr.-ft. ² °F	Percent Difference
20,300	294	2,510	2,490	+0.8
20,300	683	2,800	2,490	+12.45
19,200	297	2,480	2,430	+2.0
19,200	672	2,820	2,430	+16.1
15,900	322	2,550	2,280	+11.9
15,900	875	2,900	2,280	+27.2
11,900	246	3,030	2,080	+45.7
11,900	552	3,450	2,080	+65.9

TABLE VI
PRESSURE DROP RESULTS

Run Number	ΔP ft. H ₂ O	V_m ft./sec.	T °F	Re	$f = \frac{\Delta P g_c \rho}{2 G^2 N}$
P1	1.32	6.25	75.5	23,100	0.0613
P2	1.03	5.84	75.5	21,600	0.0620
P3	1.03	5.21	75.6	19,200	0.0695
P4	.85	4.89	75.6	18,100	0.0645
P5	.685	4.13	75.6	15,200	0.0723
P6	.525	3.46	75.7	12,800	0.0788
P7	.417	2.92	75.7	10,800	0.0879
P8	.290	2.33	75.8	8,670	0.0969
P9	.180	1.78	75.8	6,600	0.103
P10	.100	1.24	75.9	4,600	0.118

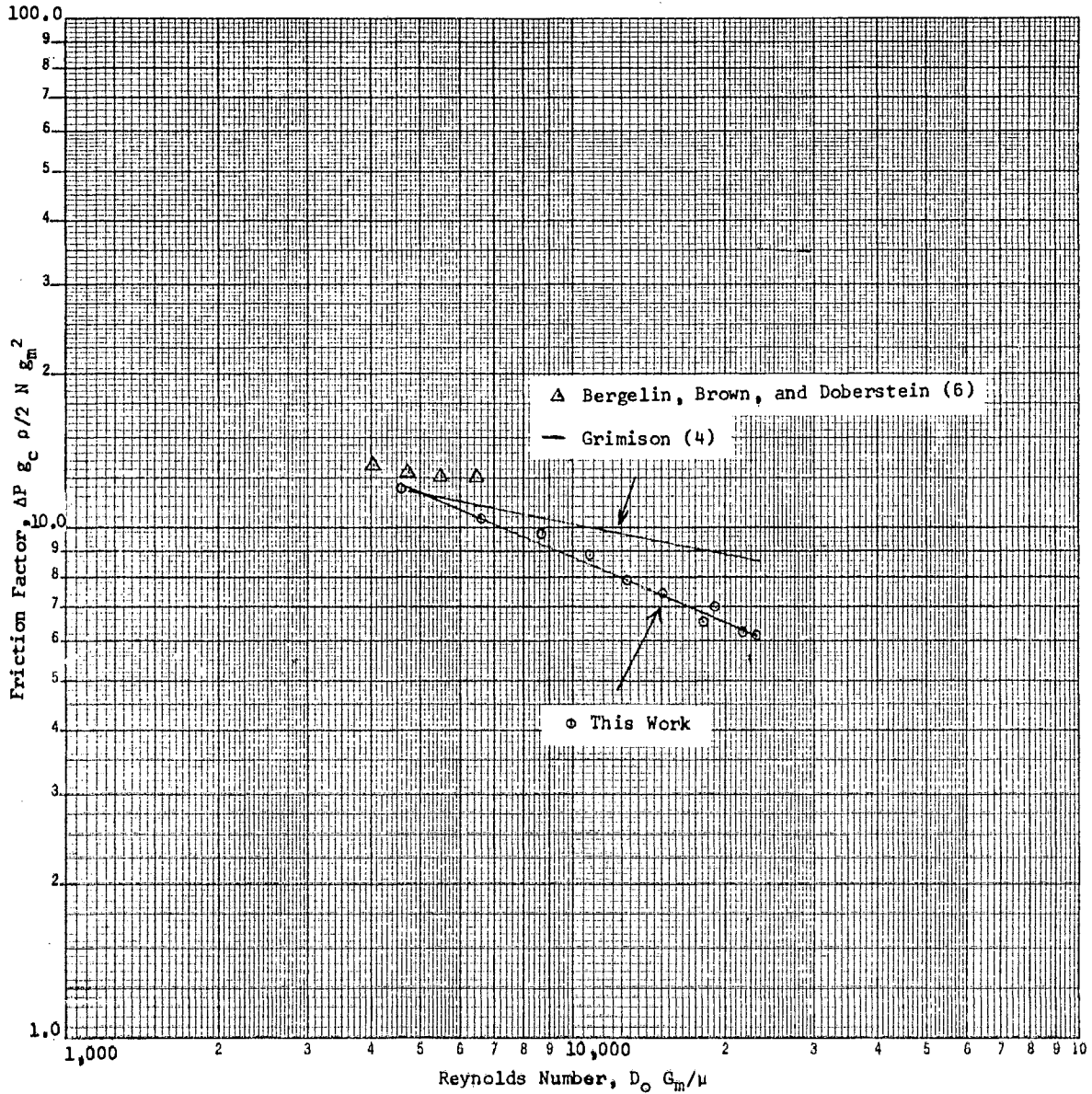


Figure 11. Friction Factor Versus Reynolds Number for a Tube Bank Having a Rotated Square Tube Configuration and a Pitch Ratio of 1.33

TABLE VII
COMPARISON OF FRICTION FACTOR RESULTS WITH
GRIMISON CORRELATION (4)

Re	f (This Work)	f (Grimison)	Percent Difference
23,100	0.0613	0.085	-27.9
21,600	0.0620	0.086	-27.9
19,200	0.0695	0.088	-21.0
18,100	0.0645	0.090	-28.4
15,200	0.0723	0.094	-23.1
12,800	0.0788	0.098	-19.6
10,800	0.0879	0.102	-13.9
8,670	0.0969	0.107	-9.43
6,600	0.103	0.110	-6.36
4,600	0.118	0.118	0.0

CHAPTER VII

CONCLUSIONS AND RECOMMENDATIONS

Conclusions

Neither of the tube designs gave satisfactory results for the heat transfer coefficients of water; thus, no non-Newtonian fluid measurements were made.

The apparatus gave reproducible friction factor data. These data were in good agreement with literature values in the Reynolds number region (4,000 to 8,000) where there are two literature sources of data for comparison. In the Reynolds number region where there is one literature source for comparison, these data do not agree with the literature values.

The difficulties in getting acceptable heat transfer data are largely due to conduction of heat to the walls of the tube bank. Some difficulty was also caused by the fact that the tube bank was too small to permit proper instrumentation.

Recommendations

It is recommended that future studies of this type be carried out using larger equipment. It is also recommended that a two-fluid system be used; that is, a fluid such as steam or cold water should be used in the tubes instead of electrical heating. This would eliminate the problem of measuring the tube wall temperature. The work would perhaps be more applicable to commercial use where a large number of tubes are providing or removing heat instead of a single tube.

A SELECTED BIBLIOGRAPHY

1. Wilkinson, W. L. Non-Newtonian Fluids. Chapter 1. New York: Pergamon Press, 1960.
2. Pierson, O. L. "Experimental Investigation of the Influence of Tube Arrangement on Convection Heat Transfer and Flow Resistance in Cross Flow of Gases Over Tube Banks." Transactions A.S.M.E., 59 (1937), 563.
3. Huges, E. C. "Experimental Investigation of Effects of Equipment Size on Convection Heat Transfer and Flow Resistance in Cross Flow of Gases Over Tube Banks." Transactions A.S.M.E., 59 (1937), 573.
4. Grimison, E. D. "Correlation and Utilization of New Data on Flow Resistance and Heat Transfer for Cross Flow of Gases on Tube Banks." Transactions A.S.M.E., 59 (1937), 583.
5. Bergelin, O. P., A. P. Colburn, and H. L. Hull. "Heat Transfer and Fluid Friction During Viscous Flow Across Banks of Tubes." University of Delaware Engineering Experiment Station Bulletin No. 2, 1950.
6. Bergelin, O. P., G. A. Brown, and S. C. Doberstein. "Heat Transfer and Fluid Friction During Flow Across Banks of Tubes." Transactions A.S.M.E., 74 (1952), 953.
7. Metzner, A. B. and J. C. Reed. "Flow of Non-Newtonian Fluids-- Correlation of the Laminar, Transition, and Turbulent-Flow Regions." A.I.Ch.E. Journal, 1 (1955), 434.
8. Rabinowitsch, B. Z. Physik Chem., 145A (1929), 1.
9. Acrivos, A., E. E. Petersen, and M. N. Shah. "Heat Transfer from a Cylinder to a Power-Law Non-Newtonian Fluid." A.I.Ch.E. Journal, 8 (1962), 542.
10. Albertson, Maurice L., et al. Fluid Mechanics for Engineers. Englewood Cliffs, New Jersey: Prentice-Hall (1960), 562.
11. Perry, J. H. Chemical Engineers' Handbook. New York: McGraw-Hill Book Company (1950).

APPENDIX A

DEFINITION OF SYMBOLS

- A_F - Minimum cross-sectional area for flow
- A_N - Tube area for heat transfer
- D - Tube diameter
- D_O - Outside diameter of tube
- D_M - Orifice manometer reading
- D_T - Tube bank manometer reading
- F - Time to collect 21 lb. water for orifice calibration
- f - Fanning friction factor
- G - Mass velocity
- G_m - Maximum mass velocity
- g_c - Conversion factor, 4.18×10^8 (lb._m-ft.)/(lb._f-hr.²)
- h - Heat transfer coefficient
- K' - Consistency index for the generalized equation
- L - Tube length
- N - Number of tube rows
- n - Flow index for the power-law equation
- n' - Flow index for the generalized equation
- P - Pressure
- Q - Heat duty
- R - Radius
- Re - Reynolds number
- T - Temperature
- u - Velocity
- V - Bulk average velocity
- V_m - Maximum velocity occurring at minimum cross-sectional area
- W - Mass flow rate
- $\frac{du}{dy}$ - Shear rate

$\left(\frac{du}{dy}\right)_w$ - Shear rate at the wall

ΔP - Pressure drop

τ - Shear stress

τ_y - Initial shear stress for Bingham plastic

μ - Viscosity

μ_B - Plastic viscosity

θ - Angle from forward stagnation point in the clockwise direction

ρ - Density

APPENDIX B

EXPERIMENTAL AND CALCULATED DATA

TABLE VIII
HEAT TRANSFER RAW DATA FOR DESIGN B

Run Number	θ	Voltmeter Reading Volts	Ammeter Reading Amperes	Water Temperature °F	Tube Temperature °F	Orifice Manometer Reading in.
1	0°	15.6	0.384	75.5	87.5	24.0
2	0°	15.6	0.378	75.5	87.3	7.6
3	0°	15.6	0.380	76.0	87.5	6.2
4	90°	15.6	0.345	77.5	89.1	24.0
5	90°	15.6	0.345	77.5	88.8	15.0
6	90°	15.6	0.345	77.5	89.1	6.2
7	180°	15.6	0.338	77.0	85.5	11.6
8	180°	15.6	0.333	77.0	85.4	15.5
9	180°	15.6	0.326	77.0	85.2	6.2
10	270°	15.6	0.303	77.4	80.7	6.2
11	270°	15.6	0.305	77.5	81.0	16.0
12	270°	15.6	0.308	77.5	81.0	24.0
13	315°	15.6	0.430	75.5	83.3	1.9
14	315°	15.6	0.427	75.5	82.7	7.0
15	315°	15.6	0.412	75.5	81.2	15.0
16	315°	15.6	0.405	75.5	81.8	24.0

θ = angle from forward stagnation point in clockwise direction

TABLE IX
LOW HEAT INPUT RAW DATA FOR DESIGN C

Run Number	Voltmeter Reading Volts	Ammeter Reading Amperes	T _{water} °F	T _{tube} °F	Orifice Manometer Reading in.
17	29.0	0.978	69.7	72.4	16.0
18	29.0	0.975	70.5	72.6	25.0
19	29.0	0.981	71.1	74.0	13.5
20	29.0	0.960	71.8	76.8	6.0

TABLE X
HIGH HEAT INPUT RAW DATA FOR DESIGN C

Run Number	Voltmeter Reading Volts	Ammeter Reading Amperes	T _{water} °F	T _{tube} °F	Orifice Manometer Reading in.
21	42.8	2.07	76.8	82.2	22.4
22	54.8	3.87	78.1	90.0	22.4
23	44.0	1.98	78.4	84.2	20.0
24	58.0	3.40	78.7	90.4	20.0
25	47.5	1.99	78.8	95.0	14.4
26	60.0	4.27	78.9	93.7	14.4
27	33.0	2.18	78.9	82.9	8.3
28	49.0	3.30	78.9	86.7	8.3

SAMPLE CALCULATIONS

Heat Transfer

The heat input was found from the voltmeter and ammeter readings as shown below.

$$Q = (\text{Volts}) (\text{Amperes}) (3.418 \text{ Btu/hr.-ampere-volt}) \quad (\text{B-1})$$

The heat transfer area for the tube was

$$A_H = \pi D_o L \quad (\text{B-2})$$

$$A_H = (\pi) (0.375 \text{ in.}) (2.5 \text{ in.}) \left(\frac{1 \text{ ft.}^2}{144 \text{ in.}^2} \right) = 0.0203 \text{ sq. ft.}$$

The heat transfer coefficient was then calculated from

$$h = \frac{Q}{A_H \Delta T} \quad (\text{B-3})$$

The velocity used in the Reynolds number was the velocity where the cross-sectional area for flow was minimum. This minimum flow area occurred between adjacent tubes in the rotated square. For the rotated square, these tubes are in different rows. The minimum flow area was

$$A_F = (7) (0.125 \text{ in.}) (2.5 \text{ in.}) \left(\frac{1 \text{ ft.}^2}{144 \text{ in.}^2} \right) = 0.0152 \text{ sq. ft.}$$

The Reynolds number was then calculated.

$$Re = \frac{D_o V_m \rho}{\mu} \quad (\text{B-4})$$

From Table VIII, page 46, run number 1

Orifice Manometer Reading = 24.0 in.

Water Temperature = 75.5°F

Tube Temperature = 87.5°F

Voltmeter Reading = 15.6 volts

Ammeter Reading = 0.384 amperes

$Q = (\text{Volts}) (\text{Amperes}) (3.418 \text{ Btu/hr.-ampere-volt})$

$Q = (15.6 \text{ volts}) (0.348 \text{ amperes}) (3.418 \text{ Btu/hr.-ampere-volt})$

$= 20.4 \text{ Btu/hr.}$

$$h = Q/A_H \Delta T = \frac{(20.4 \text{ Btu/hr.})}{(0.0205 \text{ ft.}^2) (87.5 - 75.5) \text{ }^\circ\text{F}} = 83.3 \text{ Btu/hr.-ft.}^2\text{-}^\circ\text{F}$$

From Figure 12, page 57, for $D_M = 24.0 \text{ in.}$, $V_m = 5.63 \text{ ft./sec.}$ At 75.5°F,

$\rho_{\text{H}_2\text{O}} = 62.3 \text{ lb./ft.}^3$ and $\mu = 1.874 \text{ lb./ft.-hr.}$ (10).

$$Re = \frac{D_o V_m \rho}{\mu} = \frac{(0.375 \text{ in.}) (5.63 \text{ ft./sec.}) (62.3 \text{ lb./ft.}^3)}{(12 \text{ in./ft.}) (1.874 \text{ lb./ft.-hr.})}$$

$$Re = 21,100$$

SAMPLE CALCULATIONS

Friction Factors

The tube bank pressure drop was calculated from the manometer reading as follows:

$$\Delta P = D_T (\rho_{\text{CCl}_4} - \rho_{\text{H}_2\text{O}}) \left(\frac{1 \text{ ft.}}{12 \text{ in.}} \right) \quad (\text{B-5})$$

where D_T = manometer reading in inches

The following equation was then used to calculate the friction factor:

$$f = \frac{\Delta P \ g_c \ \rho}{2 \ G^2 \ N} \quad (\text{B-6})$$

where ΔP = pressure drop, $\text{lb.}_f/\text{ft.}^2$

G = mass velocity, $\text{lb.}/\text{hr.}\text{-ft.}^2$

N = number of tube rows = 9

From Table XI, run number P1,

Tube bank manometer reading = $D_T = 26.4 \text{ in.}$

Orifice manometer reading = $D_M = 29.4 \text{ in.}$

At 76°F , the density of CCl_4 is $99.4 \text{ lb. per cubic foot (11)}$.

$$\Delta P = (26.4 \text{ in.}) (99.4 - 62.3) \text{ lb.}/\text{ft.}^3 \left(\frac{1 \text{ ft.}}{12 \text{ in.}} \right)$$

$$\Delta P = 81.7 \text{ lb.}_f/\text{ft.}^2$$

TABLE XI
TUBE BANK PRESSURE DROP RAW DATA

Run Number	Tube Bank Manometer Reading in. H ₂ O/CCl ₄	Orifice Manometer Reading in. H ₂ O/Hg	Temperature °F
P1	26.4	29.4	75.5
P2	23.2	25.1	75.5
P3	20.60	21.6	75.6
P4	17.00	17.6	75.6
P5	13.70	13.2	75.6
P6	10.50	9.6	75.7
P7	8.34	7.2	75.7
P8	5.80	4.86	75.8
P9	3.60	2.76	75.8
P10	2.00	1.40	75.9

From Figure 12, for $D_M = 29.4$ inches, $V_m = 6.26$ ft./sec.

$$G = V\rho = (6.26 \text{ ft./sec.}) (3,600 \text{ sec./hr.}) (62.3 \text{ lb./ft.}^3)$$

$$= 1.40 \times 10^6 \text{ lb./ft.}^2\text{-hr.}$$

$$f = \frac{(81.7 \text{ lb.}_f/\text{ft.}^2) (4.18 \times 10^8 \text{ lb.}_f\text{-hr.}^2) (62.3 \text{ lb.}_m/\text{ft.}^3)}{(1.40 \times 10^6 \text{ lb.}_m/\text{hr.}\text{-ft.}^2)^2 (9)}$$

$$f = 0.0613$$

$$Re = \frac{D_o V_m \rho}{\mu} = \frac{(0.375 \text{ in.}) (6.26 \text{ ft./sec.}) (62.3 \text{ lb./ft.}) (3,600 \text{ sec./hr.})}{(1.874 \text{ lb./ft.}\text{-hr.}) (12 \text{ in./ft.})}$$

$$Re = 23,100$$

APPENDIX C

ORIFICE CALIBRATION

TABLE XII
ORIFICE CALIBRATION DATA

Orifice Manometer Reading in.	F sec./21 lb.	T °F
29.4	3.55	75.5
25.1	3.80	75.5
21.6	4.27	75.6
17.6	4.57	75.6
13.2	5.40	75.6
9.6	6.40	75.7
7.2	7.60	75.7
4.86	9.50	75.8
2.76	12.48	75.8
1.40	17.90	75.9

F = time required to collect 21 pounds of water

ORIFICE CALIBRATION CALCULATION METHOD

$$W = (60 \text{ sec./min.}) (21 \text{ lb./F sec.}) (60 \text{ min./hr.}) = \frac{75,600}{F} \text{ lb./hr.}$$

A = Minimum cross-sectioned area for flow = 0.0152 sq. ft.

$$V_m = \frac{W}{\rho A} = \left(\frac{75,600}{F} \right) \text{ lb./hr.} \left(\frac{1}{0.0152 \text{ ft.}^2} \right) \left(\frac{1}{62.3 \text{ lb./ft.}^3} \right) \left(\frac{1 \text{ hr.}}{3,600 \text{ sec.}} \right) = \frac{22.1}{F}$$

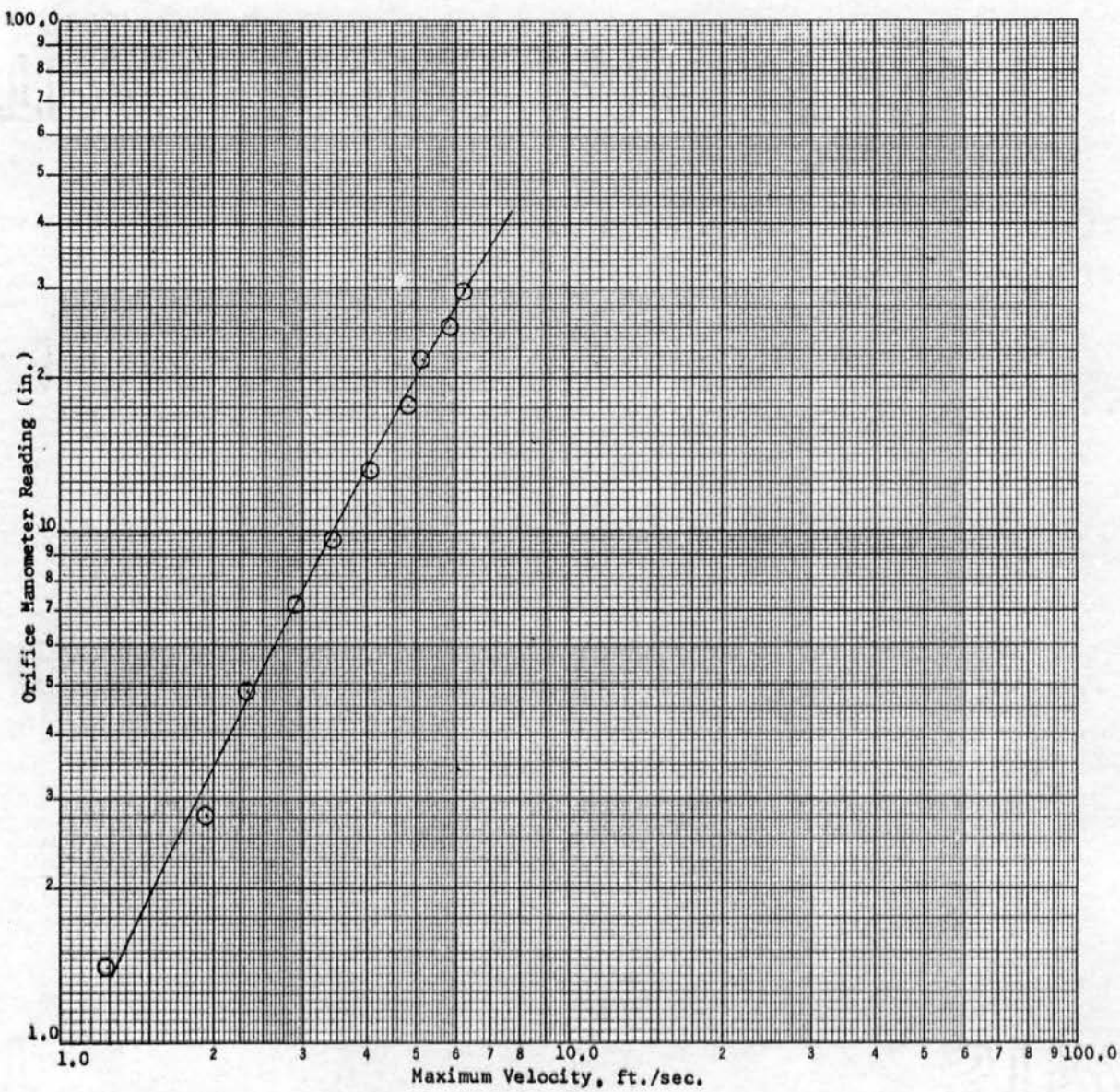


Figure 12. Orifice Calibration

VITA

Don Adams

Candidate for the Degree of

Master of Science

Thesis: HEAT TRANSFER AND PRESSURE DROP FOR FLUID FLOW ACROSS A TUBE BANK

Major Field: Chemical Engineering

Biographical:

Personal Data: Born in Oklahoma City, Oklahoma, April 2, 1940, to Water D. and Florence Hereford.

Education: Attended first two years of grade school at Lincoln School in Oklahoma City, Oklahoma; finished grade school and high school at Putnam City High School, Oklahoma City, Oklahoma; attended Oklahoma State University, Stillwater, Oklahoma, since 1958; received degree of Bachelor of Science in Chemical Engineering, May, 1962; completed requirements for Master of Science Degree in Chemical Engineering, May, 1964.

Professional Experience: Employed by Humble Oil and Refining Company, Baytown, Texas, during the summer of 1961; employed by Phillips Petroleum Company, Bartlesville, Oklahoma, during the summer of 1962.

Professional Societies: Associate Member of the American Institute of Chemical Engineers